15459

DRAFT

Glass-matrix Regolith Breccia

5854 grams

Figure 1: Photo of 15459 showing prominant clasts. Cube is 1 inch. Scale is in cm. Large clast in center is picritic basalt. Large "white" clast on east end (right side) is poikilitic impact melt studied by Ridley 1977. NASA# S75-32548. Sample has been dusted, but still has some glass patina. Lines are approximate location of saw cuts for slab (about 1975 and 1985).

Introduction

Lunar sample 15459 is a large, dense, regolith breccia from Spur Crater which has a mineral, glass and chemical composition like that of the local soil. It contains a large clast of picritic mare basalt that has been dated as 3.2 - 3.3 b.y., as well as a wide mixture of clasts of highland rock types from the Apennine Front (figure 1). The matrix contains brown glass and a mixture of glass particles with a wide range of compositions (Ridley 1975, 1977). The proportions of glass compositions closely matches that of the soil, proving that this breccia sample was produced by compaction and some fusion of local soil.

Ryder (1985) gives a nice review of what was known about 15459 as of 1985. Large pieces of this sample are used as public displays.

Petrography

Phinney et al. (1972) reported that the majority of the breccia samples from Spur Crater had a brown glass matrix; 15459 is one of these, 15465 is another (Cameron and Delano 1973). The matrix makes up about 50% of the mass and is relatively dense; 2.76 gm/cm^3 (Chung and Westphal 1973), 2.84 gm/cm^3 (Wentworth and McKay 1984; McKay et al. 1989). Micrometeorite craters can be seen in the photos of some surfaces (T1, S1)

Figure 2: Photo of sawn surface of 15459,0 after slab removed in 1985. Location of right angle cut in 1996 is shown. Scale is in cm. Large clast is picritic basalt. NASA# S85-42240.

Ridley (1975, 1977) and McKay and Wentworth (1983) classify 15459 as a regolith breccia, because it is found to contain numerous glass spheres and shards, including the green glass compositions found in abundance in the soils around Spur Crater. The bulk composition of the matrix is also very similar to that of the soil at Spur Crater (figure 3). McKay et al. (1974, 1989) classify 15459 as submature with Is/FeO = 17-27, however, relict agglutinates are hard to identify. Solar wind rare gas content is moderately high (McKay et al. 1989). The clast population is seriate (figures 2, 4, 19) and of highland, rather than mare composition. In a series of papers (Lindstrom et al. 1987, 1989, 1990; Marvin et al. 1991; Nyquist et al. 1989) report analyses of numerous small clasts mined from 15459 (see figures and tables herein). A wide variety of clasts were found; from anorthositic, to noritic, impact melt, KREEP, QMD and picritic basalt. However, clasts of quartz-normative basalt from the local mare are absent. The large clasts in 15459 (figure 1) were studied by Ridley (1975, 1977).

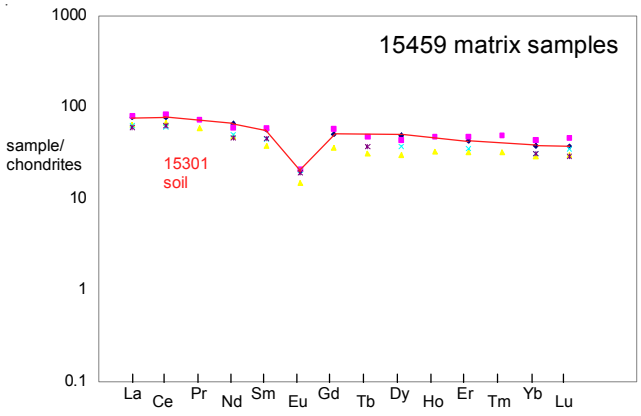

Figure 3: Rare earth composition of matrix samples of 15459 (see table 1), campared with that of soil sample 15301 from Spur crater.

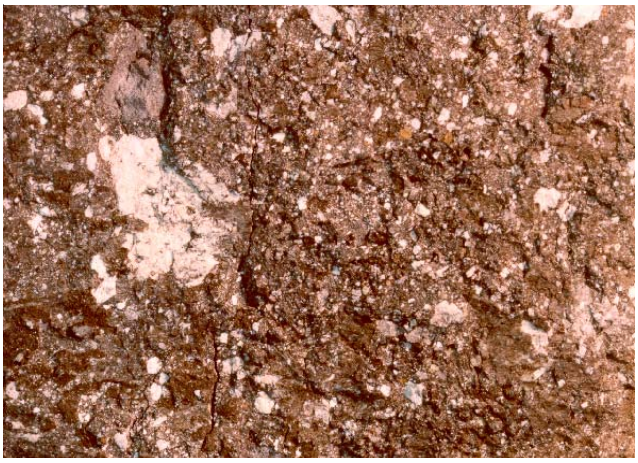

Figure 4: Close-up photo of matrix of 15459. NASA S81-34489

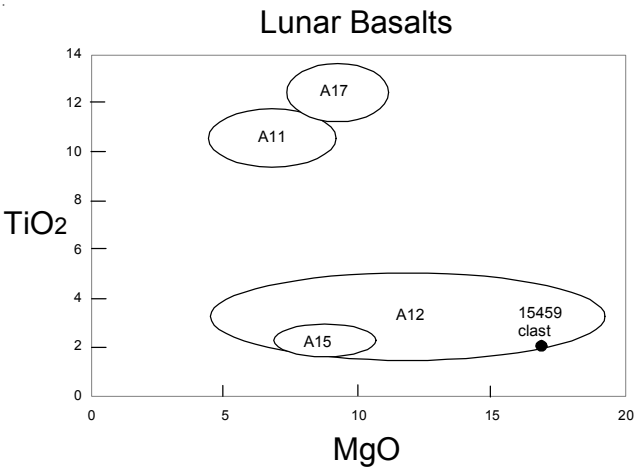

Figure 6: Data for large picritic basalt clast in 15459 compared with fields of lunar basalts.

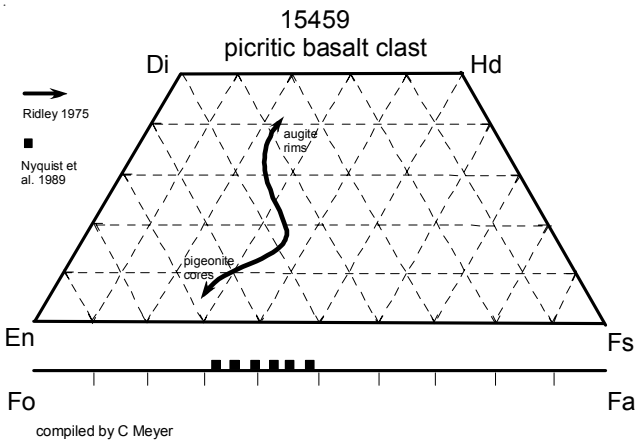

Figure 5: Olivine and pyroxene trend in large basalt clast in 15459 (a la Ridley 1975, Nyquist et al. 1989).

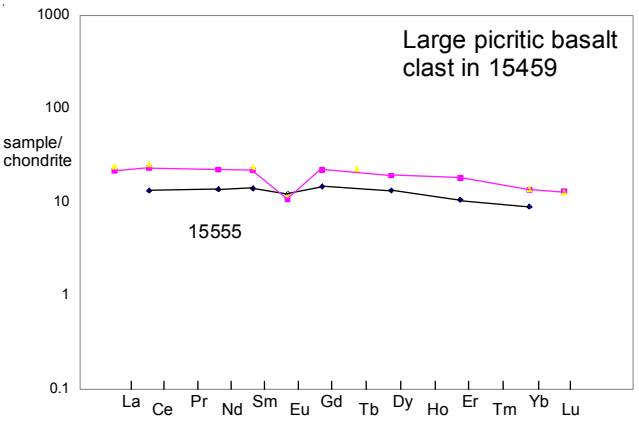

Figure 7: Normalized rare-earth-element diagram for large picritic basalt clast in 15459, compared with that of 15555 (ID, Schnetzler). The average of the 6 analyses of Nyquist et al. 1989 (INAA) compare favorably with that of Hubbard et al. 1974 (ID).

Significant Clasts

Large picritic basalt clast: The large, coarse-grained, basalt clast (figures 1 and 2) has been studied by Hubbard et al. (1974), Ridley (1975, 1977) and Nyquist et al. (1989). It is more mafic than the Apollo 15 basalts (figure 6), but with a rare-earth-element pattern like that of a basalt (figure 7). Olivine is zoned from Fo_{67} to Fo_{52}; pyroxene from $En_{70}Wo_{5}$ to $En_{40}Wo_{40}$ (Nyquist et al. 1989, Ridley 1975). The age has been determined by Ar/Ar as 3.33 b.y (Stettler et al. 1973, figure 8) and Rb/Sr as 3.22 b.y. (Nyquist et al. 1989, figure 9). This large clast measures ~ 4 x 8 x 4 cm.

The "white" poikilitic clast: This large "white" clast, seen in figure 1, has not been well documented. It is apparently a cataclastic, poikilitic highland rock with high percentage of calcic plagioclase (Ridley 1975, 1977). It may include a clast of norite (Takeda 1973). Hubbard et al. (1973), Janghorbani et al. (1973) and Ganapathy et al. (1973) provide chemical analyses (table 3a). Reid et al. (1977) picture the texture of this poikilitic clast (their fig. 1b) and considered it in their search for LKFM basalt. Pyroxenes in this clast are exsolved (ie. inverted) in a manner similar to a plutonic rock (figures 10 and 11).

White " hidden" clast: There appears to be another large white clast (hidden under the patina, figure 1) on the large piece (,184) that went to remote storage (see also figure 20). This clast may have been the one

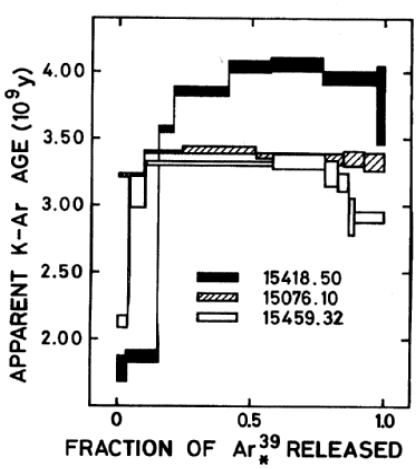

Figure 8: Argon plateau age of large basalt clast in 15459 (from Stettler et al. 1973).

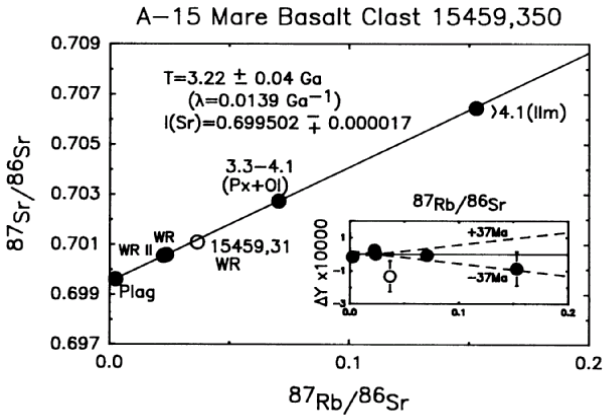

Figure 9: Rb-Sr isochron for large picritic basalt clast in 15459 (from Nyquist et al. 1989)

analyzed by Taylor et al. (1973) (,97 ?, table 3a). It is apparently otherwise unstudied.

KREEP basalt: Small fragments of KREEP basalt (sometimes mistakenly termed norite) are said to be abundant, although generally smeared-out in texture (Ridley 1975, 1977). These fragments have pyroxenes with Mg-orthopyroxene cores, zoning to ferropigeonite (figure 14). Glass of the same composition is also found in abundance in the matrix. Lindstrom et al. (1988) analyzed several clasts with this composition (table 3b, figure 15).

Quartz Monzodiorite Clast: The QMD clast (,316) in 15459 contains 2% silica, 59% plagioclase (An_{44-88}), 39% pyroxene exsolved as $En_{28}Wo_4$ and $En_{23}Wo_{41}$, with trace zircon, K-spar, ilmenite and whitlockite (Marvin et al. 1991). It has been somewhat deformed and recrystallized. Analysis by Lindstrom et al. (1988) shows high REE content (figure 15) like that of KREEP basalt, and similar to QMD from other samples (see 15405).

Ferroan Norite: Clast ,279 is a shocked and granulated norite consisting of 65% plagioclase (An_{93}), 33% pyroxene ($En_{66}Wo_2$), with rare augite ($En_{42}Wo_{45}$), ilmenite, chromite, K-spar, silica, whitlockite and zircon. Clast ,292 is a coarse-grained norite with 48% plagioclase (An_{91}), 50% pyroxene ($En_{60}Wo_3$), minor augite ($En_{41}Wo_{44}$), trace ilmenite, chromite, zircon, silica, K-spar, troilite and metal. The analyses by Lindstrom et al. (1988) are plotted in figure 12.

Ferroan Anorthosite: Clast ,274 is mostly coarse plagioclase (An_{97}) with only minute pyroxene (figures 16, 17, 18). Clast ,238 is a cataclastic anorthositic norite with 61% plagioclase (An_{95-98}), 29% pyroxene ($En_{67}Wo_2$ and $En_{41}Wo_{46}$), 10% olivine (Fo_{60}), with accessory chromite and ilmenite. Trace element contents are low (figure 18), but keep the small sample size in mind.

Magnesian anorthosite: Clast ,231w is mainly plagioclase (An_{90-93}), with scattered olivine (Fo_{69-72}), and augite ($En_{47}Wo_{42}$). High Eu in this clast (figure 18) might be due to excess plagioclase.

Chemistry

The composition of the matrix of breccia 15459 is remarkably similar to that of soil 15301 from Spur Crater (figure 3).

The composition of the large picritic basalt clast is more mafic than the typical Apollo 15 basalts (figures 6 and 7, table 2).

Summary of Age Data for 15459

	Ar/Ar	Rb/Sr	
Stettler et al. 1973	3.33 ± 0.06 b.y		mare basalt
Nyquist et al. 1989		3.22 ± 0.04	mare basalt

Note: Beware use of old decay constants.

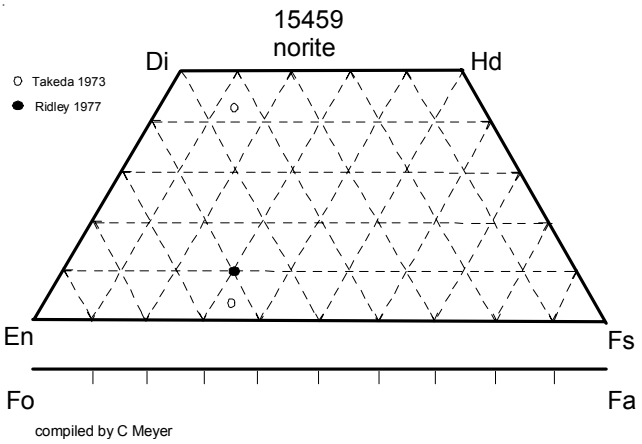

Figure 10: Pyroxene composition of norite clast in 15459 showing "inverted pigeonite" (from Takeda 1973, Ridley 1977 and Reid et al. 1977).

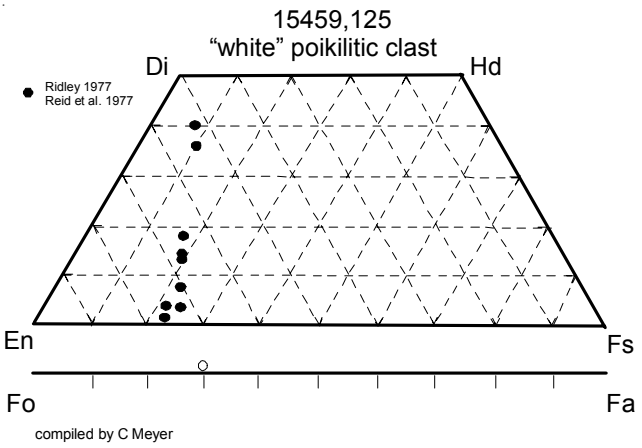

Figure 11: Pyroxene and olivine composition of large white clast in 15459 (Ridley 1977, Reid et al. 1977).

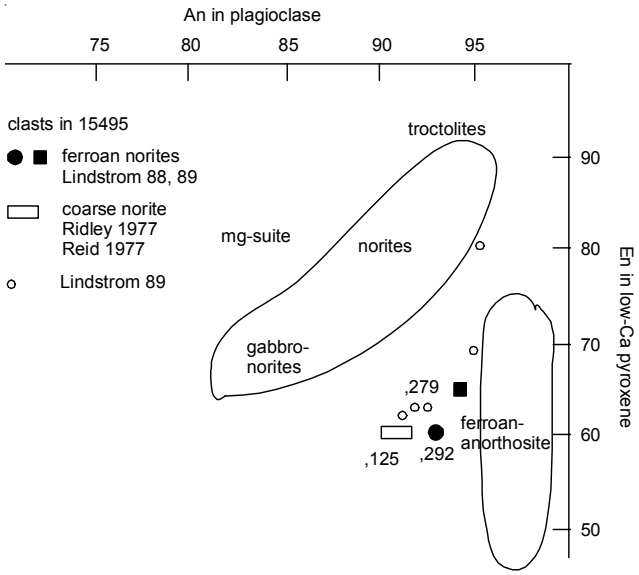

Figure 12: Plagioclase and pyroxene composition for norite clasts in 15459 (data from Marvin et al. 1988 and Ridley 1977).

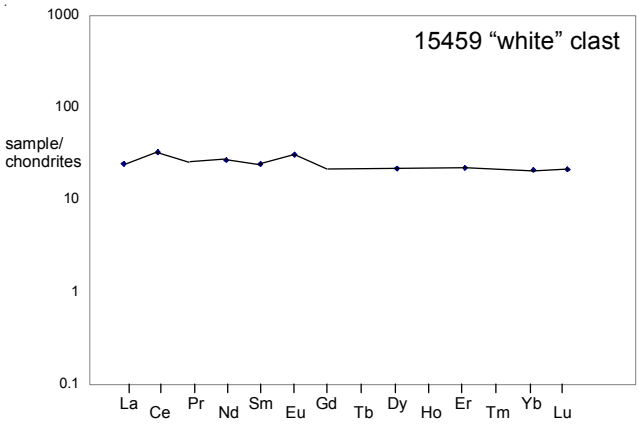

Figure 13: Normalized rare-earth-element diagram for large "white" clast in 15459 (data from Hubbard et al. 1973).

Radiogenic age dating

Stettler et al. (1973) and Nyquist et al. (1989) have dated the large picritic mare basalt clast in 15459 (figures 8 and 9). These ages are not concordant, possibly because of the reheating during breccia formation (time, temperature unknown).

Cosmogenic isotopes and exposure ages

Stettler et al. (1973) determined an exposure age of 520 m.y. by the ^{38}Ar method.

Keith et al. (1972) reported cosmic ray activity as ^{26}Al = 120 dpm/kg., ^{22}Na = 39 dpm/kg., ^{54}Mn = 16 dpm/kg., ^{56}Co = 8 dpm/kg. and ^{46}Sc = 3.9 dpm/kg.

Processing

15459 was originally studied by a consortium led by Paul Gast (see Ridley 1975, 1977).

Figure 20 illustrates the main aspects of the break-up of 15459 for allocation and displays. A large piece (,6 = 160 grams) was removed from the west end for display (figure 23). Another piece was removed, by wire saw, from the east end (,55 – 92) that included part of the "white" poikilitic clast analyzed by Taylor et al. (1973) and Hubbard et al. (1973).

In 1975 a saw cut was made thru the middle of the sample to create a large piece (,184 = 1276 grams) for remote storage, and another display (,173 = 86 grams). In 1985, a slab was cut, with many allocations of small clasts to Lindstrom and Marvin (described herein).

Additional cuts were made of the large piece in 1996, to prepare a large display sample (,447) for the U.S. National Museum at the Smithsonian Institution in Washington DC (see location of cuts in figure 2).

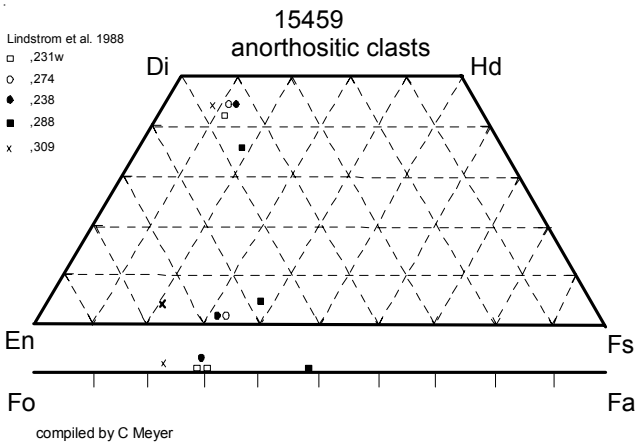

Figure 16: Pyroxene and olivine composition in ferroan and mg-anorthosite clasts in 15459 (from Lindstrom 1988).

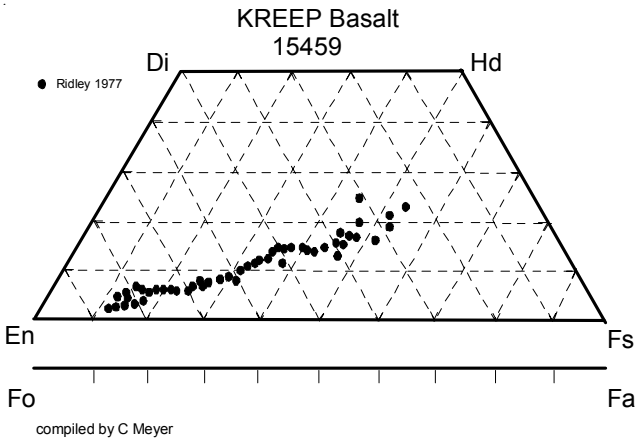

Figure 14: Pyroxene composition for KREEP-norite clast in 15459 (from Ridley 1977).

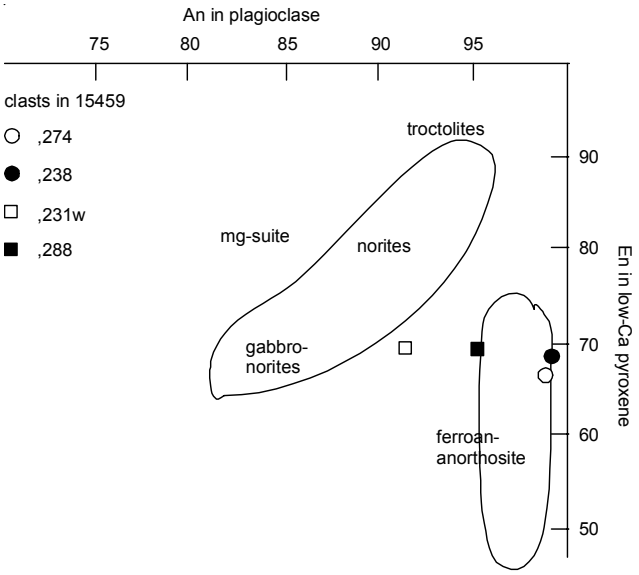

Figure 17: Plagioclase and pyroxene composition diagram for anorthosite clasts in 15459 (Lindstrom et al. 1988).

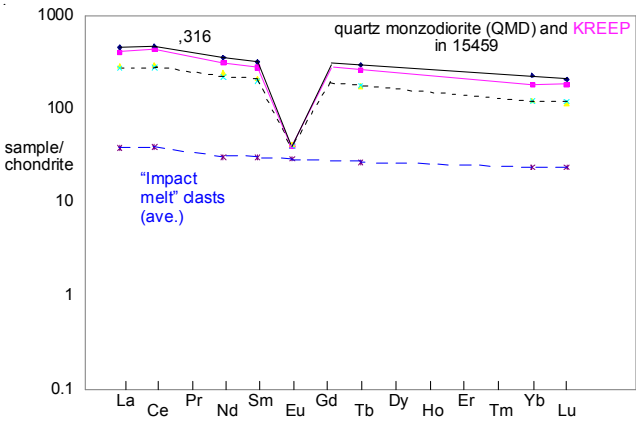

Figure 15: Normalized rare-earth-element diagram for quartz monzodiorite and KREEP clasts in 15459 compared with average of "impact melt" clasts (data from table 3).

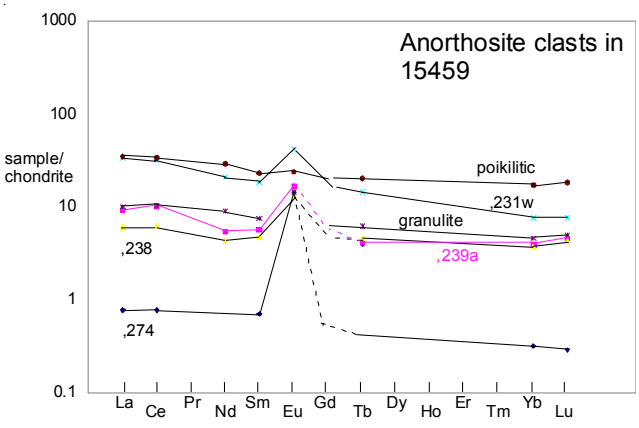

Figure 18: Normalized rare-earth-element diagram for various "anorthosite" clasts in 15459 (data from Lindstrom et al. 1988).

Table 1. Chemical composition of matrix of breccia 15459.

reference	Taylor 73			Korotev 84		Church 72 Hubbard 73		Janghorbani 73		Keith 73	
weight	,74	,97	(a)	McKay 89		Wiesmann 75		Garg 76		92 grams	
SiO2 %		46.6	(a)					45.8	(b)		
TiO2		1.02	(a)	1.11	(b)	0.911	(d)	2	(b)		
Al2O3		17.2	(a)	17	(b)			17.8	(b)		
FeO		11.2	(a)	11.6	(b)	9.4	(d)	11	(b)		
MnO		0.13	(a)	0.196	(b)			0.15	(b)		
MgO		11.4	(a)	12.3	(b)	10	(d)	11.8	(b)		
CaO		11.6	(a)	10.8	(b)	11.2	(d)				
Na2O		0.41	(a)	0.42	(b)	0.42		0.35	(b)		
K2O		0.16	(a)			0.15	(d)			0.165	(e)
P2O5											
S %											
sum											
Sc ppm	23		(a)	22	(b)			21	(b)		
V	96		(a)	73	(b)						
Cr	2150	1900	(a)	2080	(b)			1815	(b)		
Co	42		(a)	48.5	(b)						
Ni	232		(a)	213	(b)						
Cu	4.4		(a)								
Zn											
Ga	4.1		(a)								
Ge ppb											
As											
Se											
Rb	3.4	2.92	(a)			3.76	(d)				
Sr	230	160	(a)	130	(b)	130	(d)				
Y	63	46	(a)								
Zr	294	240	(a)	220	(b)	215	(d)	220	(b)		
Nb	19	15.6	(a)								
Mo											
Ru											
Rh											
Pd ppb											
Ag ppb											
Cd ppb											
In ppb											
Sn ppb	90	210	(a)								
Sb ppb											
Te ppb											
Cs ppm	0.15	0.13	(a)	0.18	(b)						
Ba	230	160	(a)	157	(b)	157	(d)				
La	19	15	(a)	14.2	(b)	14.7	(d)				
Ce	51	41	(a)	38	(b)	37	(d)				
Pr	6.5	5.3	(a)								
Nd	27	20.9	(a)	21	(b)	22.9	(d)				
Sm	8.7	5.6	(a)	6.71	(b)	6.6	(d)				
Eu	1.18	0.83	(a)	1.08	(b)	1.15	(d)	1.2	(b)		
Gd	11.5	7.1	(a)								
Tb	1.74	1.14	(a)	1.35	(b)			0.97	(b)		
Dy	10.8	7.3	(a)			9.14	(d)				
Ho	2.68	1.83	(a)								
Er	7.7	5.1	(a)			5.62	(d)				
Tm	1.2	0.78	(a)								
Yb	7.2	4.7	(a)	5.02	(b)	5.08	(d)				
Lu	1.11	0.73	(a)	0.696	(b)	0.858	(d)				
Hf	6.2	4.5	(a)	5.6	(b)	5.4	(d)	5.5	(b)		
Ta				0.68	(b)			1	(b)		
W ppb		0.12	(a)								
Re ppb											
Os ppb											
Ir ppb				5.5	(b)						
Pt ppb											
Au ppb				1.3	(b)						
Th ppm	3.71	2.52	(a)	2.4	(b)					2.9	(e)
U ppm	0.87	0.62	(a)	0.68	(b)	0.771	(d)			0.7	(e)
technique	*(a) SSMS, (b) INAA, (c) RNAA, (d) IDMS, (e) radiation counting*										

Table 2. Chemical composition of large mare basalt clast in 15459.

	big MB		splits of same big MB						*Average (6)*					
reference	Wiesmann 75				Nyquist 89				***INAA***		Ganapathy 73		Janghorbani 73	
weight	,31		188-1	188-2	240-1	240-2	409-1	409-2			,28		,29	
SiO2 %													51.1	(b)
TiO2	2	(a)	1.9			2.44				(b)				
Al2O3			6.8			5.3				(b)			5.3	(b)
FeO			23.3	24.5	23.5	24.7	21.6	21.5	***23.2***	(b)			18.7	(b)
MnO														
MgO	17.2	(a)	18.4			17.8				(b)			24.2	(b)
CaO	7.56	(a)	6.1	5.9	6.1	5.1	7.8	7.7	***6.45***	(b)				
Na2O	0.19	(a)	0.193	0.176	0.165	0.155	0.157	0.177	***0.17***	(b)				
K2O	0.039	(a)												
P2O5														
S %														
sum														
Sc ppm			26	27.7	30.8	31.7	33.2	32.2	***30.3***	(b)			43	(b)
V														
Cr			6870	6125	6850	5824	5960	6150	***6297***	(b)				
Co			76.7	78.7	76.5	77.8	72.4	72.2	***75.7***	(b)	84	(c)	69	(b)
Ni			160	120	150	120	120	150	***137***	(b)				
Cu														
Zn											0.93	(c)		
Ga														
Ge ppb											23	(c)		
As														
Se											66	(c)		
Rb	0.697	(a)									0.2	(c)		
Sr	54.9	(a)												
Y														
Zr													48.6	(b)
Nb														
Mo														
Ru														
Rh														
Pd ppb														
Ag ppb											0.34	(c)		
Cd ppb											3.2	(c)		
In ppb											0.85	(c)		
Sn ppb														
Sb ppb											0.042	(c)		
Te ppb											1.8	(c)		
Cs ppm											24	(c)		
Ba	46.7	(a)	45	55	44	66	51	61	***53.7***	(b)				
La	5.13	(a)	4.38	6.28	4.88	7.44	5.47	5.42	***5.65***	(b)				
Ce	14.2	(a)	12	18	13	20	15.1	15	***15.5***	(b)				
Pr														
Nd	10.2	(a)					8	11		(b)				
Sm	3.25	(a)	2.78	3.8	3.03	4.53	3.55	3.47	***3.53***	(b)				
Eu	0.611	(a)	0.64	0.72	0.61	0.8	0.633	0.663	***0.68***	(b)			0.67	(b)
Gd	4.4	(a)												
Tb			0.66	0.9	0.78	1.16	0.72	0.72	***0.82***	(b)			2	(b)
Dy	4.72	(a)												
Ho														
Er	2.92	(a)												
Tm														
Yb	2.21	(a)	1.79	2.4	2	2.75	2.27	2.22	***2.24***	(b)				
Lu	0.321	(a)	0.246	0.335	0.281	0.394	0.306	0.303	***0.31***	(b)				
Hf			1.94	2.7	2.35	3.27	2.29	2.33	***2.48***	(b)			1.17	(b)
Ta			0.27	0.46	0.4	0.54	0.345	0.393	***0.4***	(b)			990	(b)
W ppb														
Re ppb											0.0105	(c)		
Os ppb														
Ir ppb											0.09	(c)		
Pt ppb														
Au ppb											0.081	(c)		
Th ppm			0.21	0.44	0.3	0.7	0.5	0.53	***0.45***	(b)				
U ppm	0.12	(a)									0.107	(c)		
technique	*(a) IDMS, (b) INAA, (c) RNAA*													

Table 3a. Chemical composition of other clasts in breccia 15459.

	QMD ,316		"white		"white"		"white"		another white		ferroan norites					
reference	Lindstrom 88		Janghorbani 73		Hubbard 74		Ganapathy 73		Taylor 73		Lindstrom 88, 89					
weight	Marvin 91		,36		,38		,35		,97		,279	,292	,298	,364	,374	
SiO2 %			46	(a)					46.9	(d)	48.5	49.3		47.3	50.1	(e)
TiO2			2	(a)	1.7	(b)			0.32	(d)	0.25	0.31		0.22	0.37	(e)
Al2O3			20.1	(a)					23.5	(d)	22.9	16.9		20.2	11.5	(e)
FeO	12.9	(a)	7.9	(a)					5.85	(d)	6.97	10.99	8.78	6.63	14	(e)
MnO			0.12	(a)							0.142	0.201				(e)
MgO			14.6	(a)	9.8	(b)			9.43	(d)	7.35	10.03		13	13.2	(e)
CaO	11.3	(a)			12.5	(b)			13.7	(d)	13.38	11.28	10	11.2	8.96	(e)
Na2O	0.86	(a)	0.38	(a)	0.73	(b)			0.41	(d)	0.613	0.506	0.494	0.284	0.431	(e)
K2O					0.105	(b)			0.08	(d)	0.095	0.118				(e)
P2O5											0.065	0.039				(e)
S %																
sum																
Sc ppm	29.6	(a)	16	(a)							9.84	18.6	19.3	9.9	22	(a)
V																
Cr	1180	(a)	920	(a)					1640	(d)	2730	2360	2020	1890	2290	(a)
Co	10	(a)	19	(a)			20	(c)			26.4	30.1	13.7	15.6	34.2	(a)
Ni	<40	(a)									28	51				(a)
Cu																
Zn							2.1	(c)								
Ga									5.69							
Ge ppb							8.9	(c)								
As																
Se							50	(c)								
Rb	46	(a)			1.69	(b)	0.27	(c)	0.78	(d)		9				(a)
Sr	190	(a)			205	(b)					160	120	140	135	132	(a)
Y									30	(d)						
Zr	1510	(a)	116	(a)							120	50				(a)
Nb																
Mo																
Ru																
Rh																
Pd ppb																
Ag ppb							0.48									
Cd ppb							7.8									
In ppb							0.63									
Sn ppb									120	(d)						
Sb ppb							0.11									
Te ppb							6.4									
Cs ppm	1.25	(a)					0.106	(c)			0.12	0.13				(a)
Ba	1100	(a)			119	(b)			101	(d)	140	110	220	161	96	(a)
La	108	(a)			5.8	(b)			8.8	(d)	5.77	4.46	15.9	2.25	4.49	(a)
Ce	280	(a)			19.9	(b)			24	(d)	16.6	14.5	43.5	6.01	12	(a)
Pr									3	(d)						
Nd	160	(a)			12.2	(b)			12.2	(d)	7.7	5.5				(a)
Sm	47.2	(a)			3.6	(b)			3.2	(d)	2.29	2.98	7.55	1.04	3.2	(a)
Eu	2.26	(a)	1.9	(a)	1.74	(b)			1.06	(d)	1.4	1.78	1.29	0.75	1.49	(a)
Gd									3.7	(d)						
Tb	10.7	(a)	2.9	(a)					0.6	(d)	0.53	0.92	1.68	0.254	0.91	(a)
Dy					5.37	(b)			4.4	(d)						
Ho									0.99	(d)						
Er					3.56	(b)			2.8	(d)						
Tm									0.34	(d)						
Yb	36.9	(a)			3.44	(b)			2.3	(d)	2.33	5.15	6.79	1.36	6.12	(a)
Lu	5.07	(a)			0.523	(b)			0.32	(d)	0.36	0.78	1.04	0.19	0.91	(a)
Hf	36.5	(a)	2.97	(a)					1.6	(d)	2.63	1.05	6.96	0.72	1.27	(a)
Ta	4.77	(a)	0.89	(a)							0.48	0.058	0.87	0.061	0.068	(a)
W ppb									90	(d)						
Re ppb							0.109	(c)								
Os ppb																
Ir ppb	<4	(a)					2.2	(c)								
Pt ppb																
Au ppb	<7	(a)					0.2	(c)								
Th ppm	22.3	(a)							1.03	(d)	1.23	0.15	2.9	0.12	0.23	(a)
U ppm	6.4	(a)			0.35	(b)	0.42	(c)	0.29	(d)	0.6	0.05	0.96	0.08	0.06	(a)
technique	*(a) INAA, (b) IDMS, (c) RNAA, (d) SSMS, (e) fused bead*															

Table 3b. Chemical composition of additional lithic clasts in 15459.

	"impact melts"			KREEP			Anorthosite				Granulite	Poikilitic	
reference	Lindstrom 90			Lindstrom 88			Lindstrom 88						
weight	,414	"mean"		,242	,290	,241	,274	,239a	,238	,231w	,288	,309	
SiO2 %	44.7	45.3	(b)										
TiO2	1.7	1.77	(b)	1.74		1.7			0.17				
Al2O3	20.9	19.9	(b)	15.3		15.1		27.8	24.2	30.7			
FeO	7.94	7.82	(b)	10.9	9.51	10.9	0.226	1.71	6.27	1.51	4.22	5.82	(a)
MnO													
MgO	10.8	10.7	(b)	10.5		13.7		1.5	6.1	1.8			
CaO	12.3	12.04	(b)	9.8	11.8	11.2	19	17	15.1	17.4	16.3	12.6	(a)
Na2O	0.61	0.62	(b)	0.62	0.811	0.563	0.334	0.452	0.297	1.02	0.38	0.58	(a)
K2O	0.1	0.1	(b)		0.19								
P2O5	0.07	0.07	(b)										
S %													
sum													
Sc ppm	15.7	17.4	(a)	20.8	19.1	23.4	0.676	3.46	11.9	3.53	6.6	7.17	(a)
V													
Cr	980	1121	(a)	1410	1450	1710	26	520	740	170	390	660	(a)
Co	19	20.3	(a)	20.5	23.5	38.7	0.235	6.6	14.4	5	6	18	(a)
Ni	81	75	(a)	120	170	370		145	65	35	<40	88	(a)
Cu													
Zn													
Ga													
Ge ppb													
As													
Se													
Rb				22	17	16	0.36						(a)
Sr	205	201	(a)	140	190	200	170	150	150	340	170	170	(a)
Y													
Zr				1170	990	770		110		50	40	100	(a)
Nb													
Mo													
Ru													
Rh													
Pd ppb													
Ag ppb													
Cd ppb													
In ppb													
Sn ppb													
Sb ppb													
Te ppb													
Cs ppm				1.27	0.55	0.6	0.1	0.5	0.11	0.14	0.034	0.073	(a)
Ba	115	134	(a)	840	660	600	7.2	80	28	140	30	160	(a)
La	7.47	9	(a)	95	67.7	64.6	0.183	2.16	1.43	8.03	2.36	8.35	(a)
Ce	19.1	23.5	(a)	260	181	168	0.47	6.1	3.8	19.7	6.26	20.7	(a)
Pr													
Nd	10	13.9	(a)	140	110	100		2.37	2	9.4	4.1	13	(a)
Sm	3.81	4.49	(a)	40.7	31.3	29.6	0.105	0.84	0.71	2.72	1.12	3.41	(a)
Eu	1.57	1.64	(a)	2.18	2.34	2.26	0.8	0.94	0.74	2.37	0.82	1.34	(a)
Gd													
Tb	0.9	0.98	(a)	9.4	6.42	6.52	0.143	0.151	0.166	0.53	0.224	0.74	(a)
Dy													
Ho													
Er													
Tm													
Yb	3.39	3.91	(a)	29.5	20.1	19.8	0.052	0.63	0.61	1.24	0.75	2.8	(a)
Lu	0.489	0.58	(a)	4.42	2.76	2.94	0.007	0.112	0.104	0.187	0.119	0.448	(a)
Hf	2.94	3.53	(a)	33.4	24	22.7	0.029	1.65	0.55	1.42	0.74	2.65	(a)
Ta	0.53	0.58	(a)	4.35	2.5	2.19	0.005	0.12	0.37	0.216	0.11	0.395	(a)
W ppb													
Re ppb													
Os ppb													
Ir ppb	2.5	1.7	(a)	2.4	4.6	5.3			1.8				(a)
Pt ppb													
Au ppb				2.2	2.2								
Th ppm	1.32	1.63	(a)	22	10.5	9.55	0.005	0.23	0.14	0.76	0.258	0.83	(a)
U ppm	0.33	0.44	(a)	5.9	2.6	2.9		0.06		0.21	0.064	0.17	(a)
technique	*(a) INAA (b) elec. probe, fused beads*												

Figure 19: Photo of top side of 15459 showing zap pits, prominant clasts and marbled region on west end. NASA S75-32546. Cube is 1 inch. Location of ,6 used for public display is estimated.

Other Studies

Collinson et al. (1972, 1973)	magnetics
Brecher et al. (1975, 1976)	magnetics
Tittmann et al. (1972)	sonic velocity
Chung and Westphal (1973)	density, electrical properties
Adams and McCord (1972)	reflectance spectra
Moore et al. (1972)	C
Friedman et al. (1972)	H, C isotopes
MacDougall et al. (1973)	solar flare tracks
Bhattacharya et al. (1975)	tracks
McKay et al. (1989)	rare gas isotopes

List of Photo #s 15459

S71-44181 dust covered
S71-44176 presawing
S72-51832 B&W display ,6
S75-32546 T1
S75-32550 dusted
S81-34486
S81-34489 close-up
S75-32548 dusted
S75-32808 sawn surface
S85-42239
S85-42240 sawn surface
S85-42243 slab
S85-42242
S87-34934
S88-43662 slab distribution

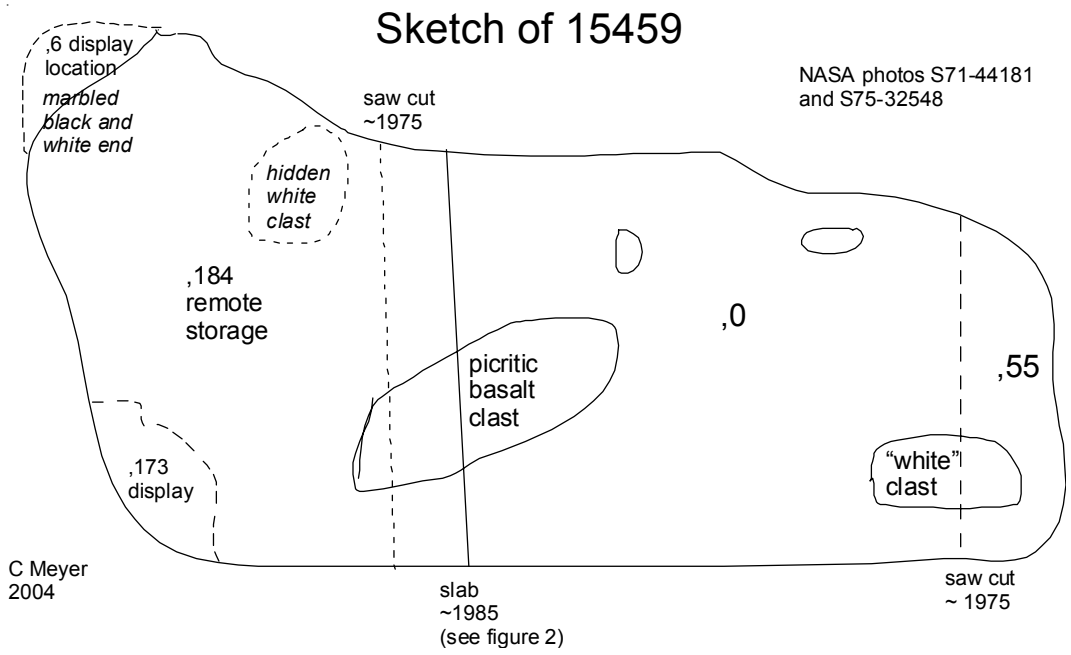

Figure 20: Sketch of 15459 (see figure 1) illustrating what is known about the processing of 15459.

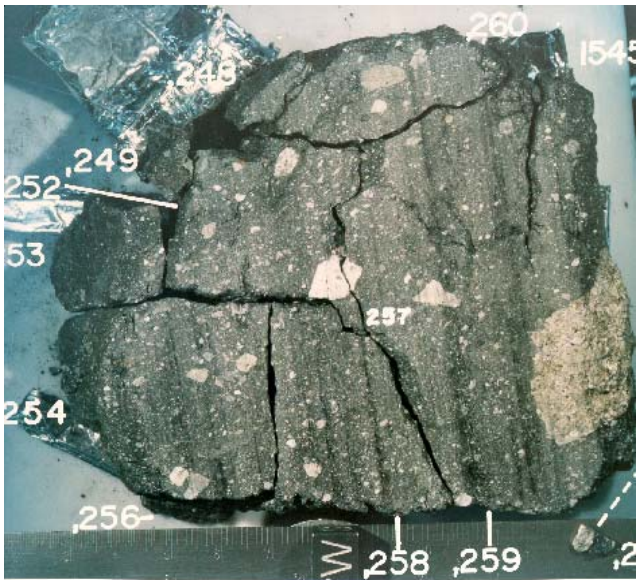

Figure 21: Front of slab, saw cut ~1975 (see location in figure 1). NASA # S85-42242.

Figure 22: Back of slab, saw cut ~ 1985 (see matching face in figure 2). NASA #85-42243.

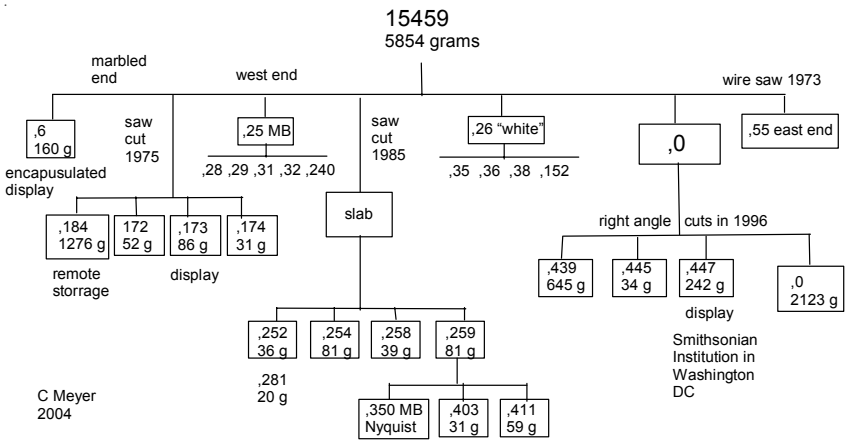

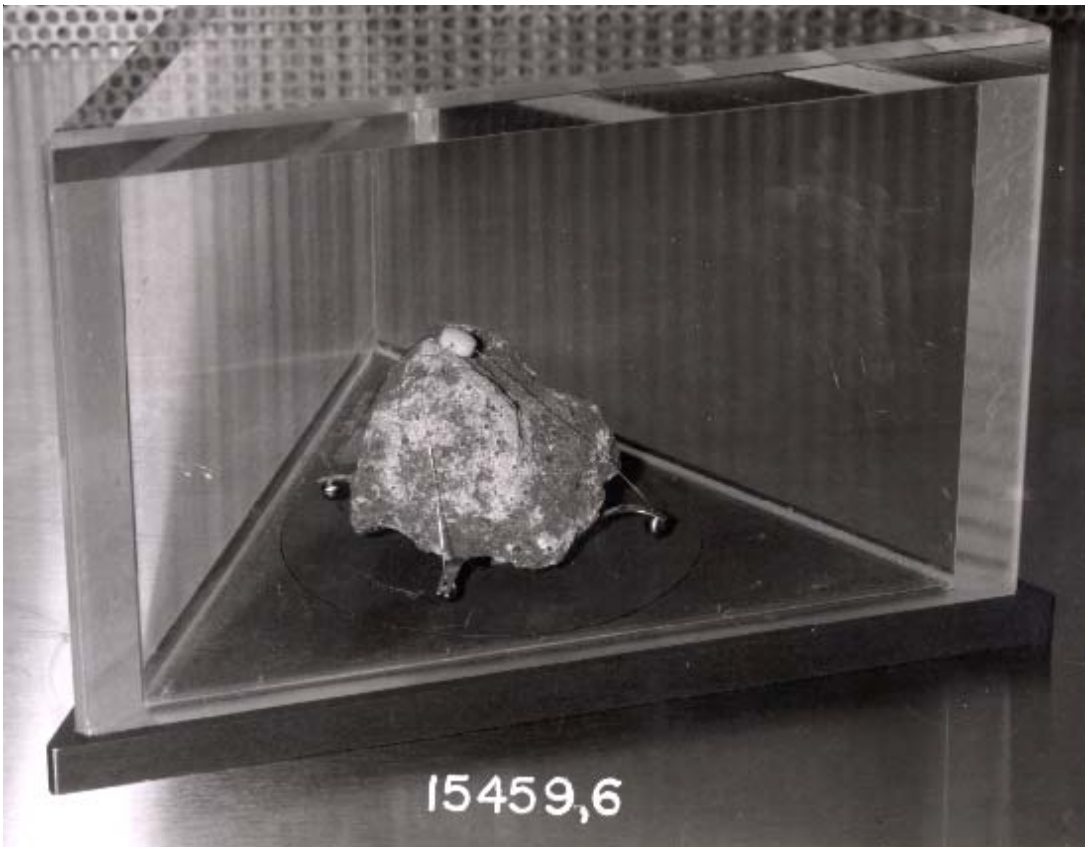

Figure 23: West end display containing marble cake lithology (now mounted in plastic).

References for 15459

Adams J.B. and McCord T.B. (1972) Optical evidence for average pyroxene composition of Apollo 15 samples. In **The Apollo 15 Lunar Samples**, 10-13. Lunar Planetary Institute, Houston.

Bhattacharya S.K., Goswami J.N., Lal D., Patel P.P. and Rao M.N. (1975) Lunar regolith and gas-rich meteorites: Characterization based on particle tracks and grain-size distributions. *Proc. 6th Lunar Sci. Conf.* 3509-3526.

Brecher A. (1975) Textural remanence: A new model of lunar rock magnetism (abs). *Lunar Sci.* **VI**, 83-85. Lunar Planetary Institute, Houston.

Brecher A. (1976a) Textural remanence: A new model of lunar rock magnetism. *Earth Planet. Sci. Lett.* **29**, 131-145.

Collinson D.W., Stephenson A. and Runcom S.K. (1973) Magnetic properties of Apollo 15 and 16 rocks. *Proc. 4th Lunar Sci. Conf.* 2963-2976.

Collinson D.W., Runcom S.K. and Stephenson A. (1975) On changes in the ancient lunar magnetic field intensity (abs). *Lunar Sci.* **VI**, 158-160. Lunar Planetary Institute, Houston.

Collinson D.W., Stephenson A. and Runcorn S.K. (1977) Intensity and origin of the ancient magmatic field. *Phil. Trans. Roy. Soc. London* **A285**, 241-248.

Friedman I., Hardcastle K.G. and Gleason J.D. (1972) Isotopic composition of carbon and hydrogen in some Apollo 14 and 15 samples. In **The Apollo 15 Lunar Samples**, 302-305. Luny Planet. Instit. Houston.

Ganapathy R., Morgan J.W., Krahenbuhl U. and Anders E. (1973) Ancient meteoritic components in lunar highland rocks: Clues from trace elements in Apollo 15 and 16 samples. *Proc. 4th Lunar Sci. Conf.* 1239-1261.

Hubbard N.J., Rhodes J.M., Gast P.W., Bansal B.M., Shih C.-Y., Wiesmann H. and Nyquist L.E. (1973b) Lunar rock types: The role of plagioclase in non-mare and highland rock types. *Proc. 4th Lunar Sci. Conf.* 1297-1312.

Hubbard N.J., Rhodes J.M., Wiesmann H., Shih C.Y. and Bansal B.M. (1974) The chemical definition and interpretation of rock types from the non-mare regions of the Moon. *Proc. 5th Lunar Sci. Conf.* 1227-1246.

Janghorbani M., Miller M.D., Ma M-S., Chyi L.L. and Ehmann W.D. (1973) Oxygen and other elemental

abundance data for Apollo 14, 15, 16 and 17 samples. *Proc. 4th Lunar Sci. Conf.* 1115-1126.

Keith J.E., Clark R.S. and Richardson K.A. (1972) Gamma-ray measurements of Apollo 12, 14 and 15 lunar samples. *Proc. 3rd Lunar Sci. Conf.* 1671-1680.

Lindstrom M.M. and Marvin U.B. (1987) Geochemical and petrological studies of clasts in Apennine Front breccia 15459 (abs). *Lunar Planet. Sci*. **XVIII**, 554-555. Lunar Planetary Institute, Houston..

Lindstrom M.M., Marvin U.B., Vetter S.K. and Shervais J.W. (1988) Apennine front revisited: Diversity of Apollo 15 highland rock types. *Proc. 18th Lunar Planet. Sci. Conf.* 169-185. Lunar Planetary Institute, Houston.

Lindstrom M.M., Marvin U.B. and Mittlefehldt D.W. (1989a) Apollo 15 Mg- and Fe-norites: A redefinition of the Mg-suite differentiation trend. *Proc. 19th Lunar Planet. Sci. Conf.* 245-254. Lunar Planetary Institute, Houston.

Lindstrom M.M., Marvin U.B., Holmberg B.B. and Mittlefehldt D.W. (1989b) Geochemistry and petrology of recrystallized gabbroic breccias from the Apollo 15 site (abs). *Lunar Planet. Sci.* **XX**, 576-577. Lunar Planetary Institute, Houston.

Lindstrom M.M., Marvin U.B., Holmberg B.B. and Mittlefehldt D.W. (1990) Apollo 15 KREEP-poor impact melts. *Proc. 20th Lunar Planet. Sci. Conf.* 77-90. Lunar Planetary Institute, Hosuton.

MacDougall D., Rajan R.S., Hutcheon I.D. and Price P.B. (1973) Irradiation history and accretionary processes in lunar and meteoritic breccias. *Proc. 4th Lunar Sci. Conf.* 2319-2336.

McKay D.S. and Wentworth S.J. (1983) A petrographic survey of regolith breccias from the Apollo 15 and 16 collection (abs). *Lunar Planet. Sci.* **XIV**, 481-482. Lunar Planetary Institute, Houston.

McKay D.S., Morris R.V. and Wentworth S.J. (1984) Maturity of regolith breccias as revealed by ferromagnetic and petrographic indicies (abs). *Lunar Planet. Sci*. **XV**, 530-531. Lunar Planetary Institute, Houston.

McKay D.S., Bogard D.D., Morris R.V., Korotev R.L., Wentworth S.J. and Johnson P. (1989) Apollo 15 regolith breccias: Window to a KREEP regolith. *Proc. 19th Lunar Sci. Conf.* 19-41. Lunar Planetary Institute, Houston.

Marvin U.B., Lindstrom M.M., Holmberg B.B. and Martinez R.R. (1991) New observations of quartz monozodiorite-granite suite. *Proc. 21st Lunar Planet. Sci. Conf.* 119-136. Lunar Planetary Institute, Houston.

Moore C.B., Lewis C.F., and Gibson E.K. (1972) Carbon and nitrogen in Apollo 15 lunar samples. In **The Apollo 15 Lunar Samples** (Chamberlain J.W. and Watkins C., eds.), 316-318. The Lunar Science Institute, Houston.

Nyquist L., Lindstrom M., Bansal B., Mittlefehldt D., Shih C.-Y. and Wiesmann H. (1989) Chemical and isotopic constraints on the petrogenesis of the large mare basalt clast in breccia 15459. *Proc. 19th Lunar Planet. Sci. Conf.* 163-174. Lunar Planetary Institute, Houston.

Reid A.M., Duncan A.R. and Richardson S.H. (1977) In search of LKFM. *Proc. 8th Lunar Sci. Conf.* 2321-2338.

Ridley W.I. (1975a) Petrology of Apollo 15 breccia 15459 (abs). *Lunar Sci.* **VI**, 671-673. Lunar Planetary Institute, Houston.

Ryder G. (1985) Catalog of Apollo 15 Rocks (three volumes). Curatoial Branch Pub. # 72, JSC#20787

Stettler A., Eberhardt Peter, Geiss J., Grogler N. and Maurer P. (1973) Ar39-Ar40 ages and Ar37-Ar38 exposure ages of lunar rocks. *Proc. 4th Lunar Sci. Conf.* 1865-1888.

Takeda H. (1973) Inverted pigeonites from a clast of rock 15459 and basaltic achondrites. *Proc. 4th Lunar Sci. Conf.* 875-885.

Taylor S.R. (1973) Geochemistry of the lunar highlands. *The Moon* **7**, 181-195.

Tittmann B.R., Housley R.M., Cirlin E.H. and Abul-Gaward M. ('1972) Rayleigh wave studies of two Apollo 15 rocks. In **The Apollo 15 Lunar Samples**, 462-465. Luny Planet. Inst. Houston.

Wentworth S.J. and McKay D.S. (1984) Density and porosity calculations for Apollo 15 and 16 regolith breccias (abs). *Lunar Planet Sci*. **XV**, 906-907.